Eur. Phys. J. D **30**, 149–153 (2004)
DOI: 10.1140/epjd/e2004-00069-3

THE EUROPEAN PHYSICAL JOURNAL D

High resolution multiphoton ionization and dissociation of acetone via 3s ← n Rydberg transitions

E. Mejía-Ospino[1,2,a], G. García[2], A. Guerrero[1], I. Álvarez[1], and C. Cisneros[1]

[1] Centro de Ciencias Físicas, Universidad Nacional Autónoma de México, Cuernavaca, Mor. Apdo. Post. 48-3, C.P. 62210, Mexico
[2] Laboratorio de Espectroscopía Atómica y Molecular, Universidad Industrial de Santander, Bucaramanga A.A.678, Colombia

Received 21 November 2003 / Received in final form 21 March 2004
Published online 11 May 2004 –

Abstract. Measurements of multiphoton ionization and dissociation of acetone are reported in the wavelength range 582.60–585.80 nm at photon energy resolution of 0.3 cm^{-1}. To our knowledge there are not available results of (3+2) REMPI on acetone at 0.01 nm in this region. The experiments were performed using an Nd:YAG-OPO (optical parametric oscillator) laser system coupled to time-of-flight mass spectrometer. The ion yield and the single ion channel are presented. The high-resolution three-photon resonance multiphoton spectrum of the acetone $3s \leftarrow n$ *Rydberg* transition is also reported. The experimental results show three dissociation channels of the acetone ion, leading to the products: (CH_3CO^+), (CH_3^+) and (COH^+); the channel $CH_3COCH_3^+ \rightarrow CH_3CO^+ + CH_3$ being the most favored. The acetone and acetyl ions are observed in all wavelength range investigated. In addition, we have measured the origin of the $3s \leftarrow n$ and $4s \leftarrow n$ transitions, and vibrational bands of the $3s$ state.

PACS. 33.80.Rv Multiphoton ionization and excitation to highly excited states (e.g., Rydberg states) – 33.15.Ta Mass spectra – 33.80.Gj Diffuse spectra; predissociation, photodissociation

1 Introduction

When a molecule is excited by multiphoton absorption, ionization and dissociation may occur. Ion yield spectroscopy provides a very detailed picture of the fragmentation processes following multiphoton excitation. The observation of the resulting ions is very informative as to the nature of the excited and ionized states and of the dynamics of fragmentation processes. Lasers combined with time-of-flight mass spectrometry is an excellent tool to examine the behavior of molecules excited by one or more photons by monitoring the ion yield of all ion fragments (total yield mode) or of the single ion channel (partial yield mode) as a function of photon energy.

Acetone is the most frequently studied molecule of its type. Being the simplest carbonyl molecule, it presents *Rydberg* states of particular interest to ion-electron reaction studies. In this paper, for first time to our knowledge, both partial yield and total yield mode are presented for three-photon resonant excitation of the $3s \leftarrow n$ *Rydberg* transition and five photon ionization spectra for acetone at photon energy resolution of 0.3 cm^{-1} in the wavelength range from 582.60 to 585.80 nm. Similar dissociation pathways were reported by Buzza et al. [5].

[a] e-mail: emejia@ce.fis.unam.mx

The $3s$ [1–6] and $3p$-*Rydberg* [7–11] states have been studied using single-photon absorption multiphoton ionization as well as two-photon resonance. Philis et al. [8] resolved vibrationally the $3p$-*Rydberg* and determined the a_2 torsional mode by two-photon resonant multiphoton ionization. Kandu et al. [9] studied the methyl effects on acetone $3p$-*Rydberg* spectra and determined the torsional fundamental frequencies of a_2 and b_1 modes of the $3p$-*Rydberg* state. There are also relevant studies where the assignments for the vibrational levels of the $3p$-*Rydberg* state are reported [7,8,10,11]. Other theoretical and experimental studies [12–14] reported the excitation energy of the $3p$-*Rydberg* states: $3p_x$ (∼7.35 eV), $3p_y$ (∼7.41 eV), $3p_z$ (∼7.45 eV).

With regard the $3s$-*Rydberg* state, there are several studies about vibrational structure and the dynamics of the ionization and dissociation of acetone via excitation of the $3s$-*Rydberg* state. Gaines et al. [1] studied the single photon absorption in jet-cooled acetone to resolve the vibrational spectrum of the $3s$-*Rydberg* state. This work was carried out with resolution of 30 cm^{-1} and the results show the origin band at 51258.9 cm^{-1}. McDiarmid [3] studied the vibrational structure of the $3s$ state of acetone at −77 °C with resolution of 15 cm^{-1} and assigned the torsional fundamental frequencies. Philis and Goodman [4] resolved the vibrational modes of the $3s$ state and studied

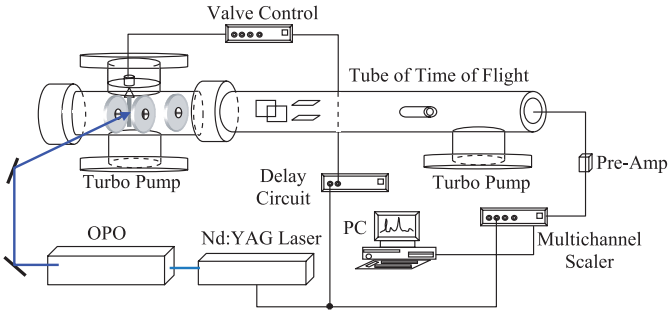

Fig. 1. Experimental arrangement.

the methyl rotational effects on acetone 3*s-Rydberg* spectra by two-photon resonant multiphoton ionization. These work reports the origin band at 51203 cm^{-1}.

Buzza et al. [5] and Zhong et al. [6] have studied the dissociation dynamics of the acetone molecule upon photoexcitation to the S_1 and 3*s-Rydberg* states using femtosecond time-resolved multiphoton ionization technique, with 585 nm photons (<100 fs) reaching the 3*s-Rydberg* state in a three-photon process.

2 Experimental

The experiments were performed using a laser-time of flight mass spectrometry system. Partial measurements of photoionization and photodissociation of acetone and the detailed description of the apparatus have been reported elsewhere [15].

A schematic diagram of the experimental apparatus is presented in Figure 1. The experimental set-up consists, basically, of the sample injection system, an Nd:YAG-OPO laser, and the time of flight spectrometer.

The acetone beam was prepared by vaporizing liquid acetone (J.T. Baker, 99.5%) about 25 °C and mixed with 1.0 atm of helium carrier gas. The gas mixture was expanded through a pulsed valve with 800 μm nozzle diameter, collimated by a skimmer of 1 mm of diameter, then introduced into the ionization region. The laser is aligned in such a way so that the molecular beam, the accelerating field, and laser beam are perpendicular to each other and intersect at the center of the electrodes. In order insure that the laser beam and the molecular beam coincide in time at the center of the electrodes plates of TOF spectrometer and that the detection and recorder system get ready to count the ions generated by the interaction between photons and molecules, a home built delay circuit was used. The interaction between the two beams was achieved in the following sequence: the first laser pulse produce a TTL signal which is introduced at the delay circuit and this generates a second TTL with a delay that can be changed to optimize the ion signal. This, in turn, is used as trigger to open the nozzle. In our system the delay is about 98.7 ms and allows the first molecular pulse to interact with the second laser pulse, which initializes other cycle. As it has been pointed out in reference [15], the open time of the valve is the 400 μs and pulse frequency is 10 Hz, same as the laser. The TTL of the laser is also used to start the Scalar Multichannel (Turbo-MCS, EG&E ORTEC) recorder.

Using an Optical Parametric Oscillator, OPO, pumped by third-harmonic of the Nd:YAG laser, laser pulses of high intensity, tunable in the range of 450–680 nm and resolution of 0.2 cm^{-1} can be generated. In this study, we used output power of 10 mJ/pulse in the 582.60–585.80 nm range. The laser beam was focused onto the interaction region by a quartz lens of focal length of 150 mm. The direction of the laser polarization was set parallel to that of the axis of the mass spectrometer. The energy per pulse was measured at the exit of the TOF with a power energy meter.

The products of the multiphoton ionization and dissociation were analyzed and collected using a time-of-flight spectrometer. The cations were accelerated to 4 keV by three parallel electrode-plates with Wiley–McLaren [16] condition so that they were spatially focused through 1m free-field region. The TOF system was pumped by two turbo molecular pumps with a pumping rate of 450 l/s, both backed up by an oil-free scroll pump. The first turbo molecular pumps are located below the interaction region while the second is in the detection region. The base pressure in the TOF spectrometer is about 4×10^{-8} Torr. When the pulsed valve is open the pressure decreases to 8×10^{-5} Torr and returns to the base pressure when closed.

The ions $CH_3COCH_3^+$, CH_3CO^+, COH^+ and CH_3^+ produced by the interaction between the laser and molecular beam are detected using a channeltron multiplier detector. The signal from the detector is amplified using a fast amplifier. The spectra were recorded by using a Scalar Multichannel recorder (Turbo-MCS, EG&E ORTEC) and were stored on a PC. The dwell time used on the MCS was 20 ns; typically 1000 channels were recorded, and a TOF spectrum usually represents 2000 laser pulses.

To calculate the resolving power of the time-of-flight spectrometer we used (4+1)REMPI of xenon at 499.05 nm. The xenon was chosen because its mass spectra is well-known and present a considerable number of isotopes. The resolution ($t/2\Delta t$) of this mass spectrometer was 490.

3 Results and discussion

3.1 Fragmentation of acetone cation

We have obtained partial and total yield for multiphoton ionization and dissociation of acetone for the following ionic species: CH_3^+, COH^+, CH_3CO^+, and $CH_3COCH_3^+$ from 582.60 to 585.80 nm. Figure 2 shows the time-of-flight spectra of acetone at 582.850 nm. The total ion yield shows four prominent peaks: m/e = 15, 29, 43 and 58 which correspond to CH_3^+, COH^+, CH_3CO^+ and $CH_3COCH_3^+$, respectively. The ions CH_3CO^+ and $CH_3COCH_3^+$ are observed for all the wavelengths used in this study even at low energy per pulse of the laser (8 mJ/pulse).

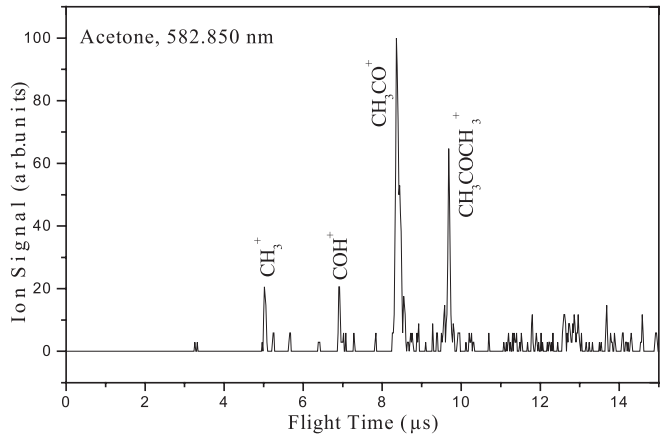

Fig. 2. Multiphoton ionization time-of-flight mass spectrum of acetone at 582.850 nm.

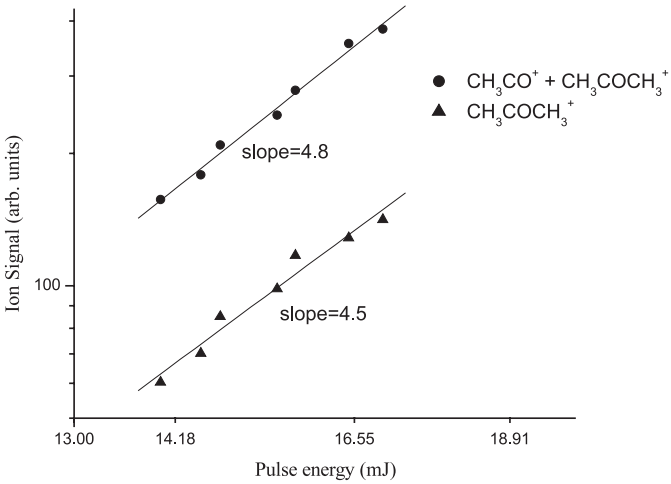

Fig. 3. Log–log plot of laser energy vs. integrated ion signal for: (•) CH_3CO^+ $CH_3COCH_3^+$ and (▲) $CH_3COCH_3^+$.

Jackson et al. and Trot et al. previously reported that the excitation energy of the 3*s-Rydberg* state is ∼6.35 eV and the ionization potential of acetone is 9.7 eV [17,18]. The photon energy used in this experiment for the multiphoton ionization of the acetone is in the range 2.116 to 2.128 eV, therefore, the ionization of the acetone is via (3+2) resonant multiphoton ionization process: three-photons to excite to the 3*s-Rydberg* state, and two photon to ionize the acetone molecule. The absorption of five photons by neutral molecule leaves the acetone ion with an excess energy of ∼0.9 eV which is sufficient to dissociate the molecular ion according to:

$$CH_3COCH_3^+ \rightarrow CH_3CO^+ + CH_3, \quad (1)$$

$$\rightarrow CH_2CO^+ + CH_4, \quad (2)$$

$$\rightarrow CH_3CO + CH_3^+. \quad (3)$$

The above dissociation channels have been reported leaving the acetone ion with an internal energy between 0.5–8 eV [17]. The reactions (1) and (3) are the most often observed channels, especially at high internal energies of the acetone ion. While it has been suggested that for low internal energies the reaction (2) is the main channel. In our work we have not observed the CH_2CO^+ ion. This suggests that at 10.6 eV in five-photons photodissociation process the methyl loss is more favorable than the methane elimination.

In addition, we have observed the presence the COH^+ ion ($m/e = 29$). Majumder et al. [19] in their study of acetone at 355 nm reported that the COH^+ ion ($m/e = 29$) is produced by the dissociation of enolic ions, $CH_2{=}COH^+$. However the COH^+ ion can be originated by keto-enol tautomerism the either $CH_3COCH_3^+$ or CH_3CO^+ ion accordingly to the reactions (4) and (5) [19–21]:

$$CH_3CO^+ \rightarrow CH_2{=}COH^+$$

$$\rightarrow COH^+ + CH_2, \quad (4)$$

$$CH_3COCH_3^+\bullet \rightarrow CH_3C(OH){=}CH_2^+\bullet$$

$$\rightarrow CH_2{=}COH^+ + CH_3\bullet$$

$$\rightarrow COH^+ + CH_2. \quad (5)$$

In the spectra, two broad structures are present, one around $m/e = 43$ and other around $m/e = 58$ at all wavelengths used. The maximum around $m/e = 43$ can be interpreted as the interference of two different channels: CH_3CO^+ and CH_2COH^+, i.e. reaction (4). In the same way the observation of broadening around $m/e = 58$ is interpreted as a keto-enol transformation of the molecular ion reaction (5). The keto-enol tautomerization is a well-known bimolecular process in solution [20]. In contrast, in the gas phase, the unimolecular isomerization of ionized ketone or aldehyde into its enolic counterpart does not occur spontaneously since a high-energy barrier separates the keto radical cation and its enol counterpart. It is been observed that some neutral molecules can catalyze the conversion of carbonyl ions into their more stable enolic counterpart [20,21]. Mourgues et al. [21] have found that acetone itself can be a good catalyst to promote keto-enol tautomerization of acetone radical cation. Based on Mourgues's conclusions, we interpret that the observation of bimodal velocity distribution at $m/e = 58$ is due to the production of ionized enol, $CH_3C(OH)CH_2^+$, catalyzed by neutral acetone into the interaction region.

In order to estimate the number of photons involved in the ionization of acetone, we have measured the energy dependence of acetone and acetyl plus acetone ions at 585.60 nm (Fig. 3). The input energy of the laser covers a range from 13 to 17 mJ. In this figure, the logarithm of the relative intensity of the ion peak is plotted against the logarithm of the relative input laser energy. A fifth dependence is observed for the two cases. This is an evidence that acetone absorbs five photons of 585.60 nm to ionize and dissociate through the channel (1).

3.2 Three-photon 3s-Rydberg spectra of acetone

The three-photon resonance five-photon ionization 3*s-Rydberg* spectra are shown in Figure 4. Figures 4a, 4b and 4c correspond to the three-photon resonant and five-photon ionization spectra obtained by monitoring

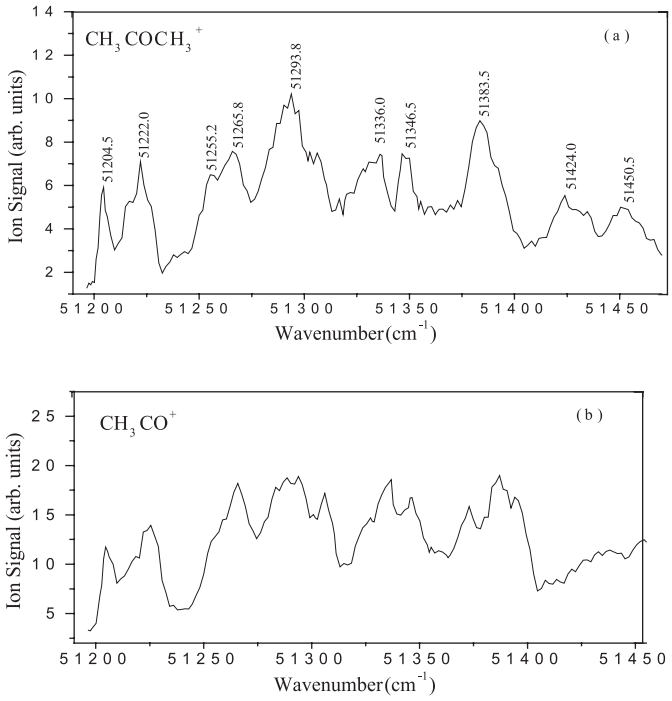

Fig. 4. Three-photon resonant multiphoton ionization spectra of the $3s \leftarrow n$ *Rydberg* transition of acetone obtained by monitoring: (a) $CH_3COCH_3^+$; (b) CH_3CO^+ and (c) $CH_3COCH_3^+$ plus CH_3CO^+.

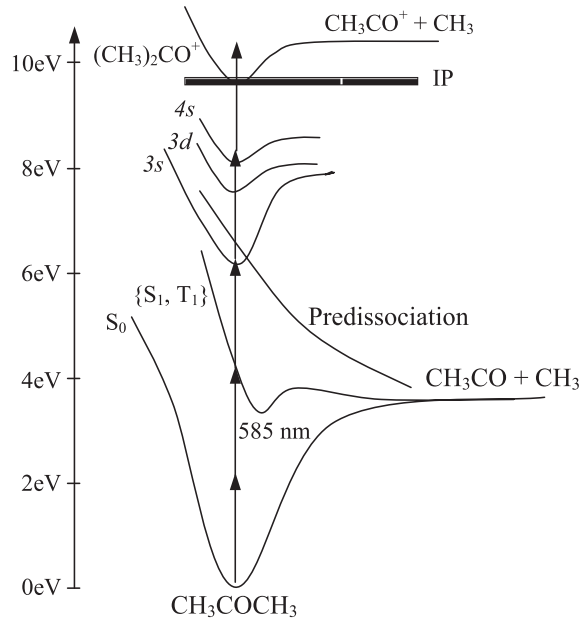

Fig. 5. Schematic representation of the potential energy surfaces. The states accessed by the photons used in this study are shown.

the acetone $CH_3COCH_3^+$, acetyl radical CH_3CO^+ and $CH_3COCH_3^+$ plus CH_3CO^+ ion signals, in the region 0–250 cm^{-1}, respectively. In previous studies, at low resolution, only the total ion yield is reported [1,3,4], the same type of results are shown in Figure 4c at high resolution and it allow resolve the vibrational structure of the 3*s*-*Rydberg* state. Wave numbers in the spectra have been corrected for vacuum.

The three spectra (Fig. 4) do not show significant differences in the overall features but there are differences in intensity. In general, the intensity obtained monitoring the acetyl ion is approximately two times higher than the intensity of the acetone ion. This difference is even observed at low laser pulse intensity (12 mJ/pulse).

In the three-photon resonant five-photon ionization spectra observed was more complex than two-photon spectra, because the energies per photon used in this study allow the excitation of both the 3*s*- and 4*s*-*Rydberg* states, resulting (3+2) and (4+1) REMPI process, respectively [6]. Figure 5 shows some of the states of acetone, which could be excited at the wavelengths used herein before ionization/dissociation occurs. It is possible to identify the origin of the 3*s* state at 51204.5 cm^{-1}. Our results are in agreement with the value obtained by Philis and Goodman [4] in the two-photon studies.

In all the spectra we observe several bands, these can be identified as the vibrational frequencies of 3*s*-*Rydberg* state and other bands, which we assume to correspond to 4*s*-*Rydberg*. The spectrum in Figure 4 has been constructed on the basis of three photon energies if we assume four-photon energy, the band at 51222.0 cm^{-1} will correspond to 68296 cm^{-1} (∼8.46 eV), which in turn is the $4s \leftarrow n$ *Rydberg* transition, in agreement with the theoretical value reported (8.53 eV) by Galosso [12]. Despite the high resolution of our experimental system (0.3 cm^{-1}), we observed bands in the spectra with FWHM ≈ 10 cm^{-1}; this can be due to the mixture of (3+1) and (4+1) REMPI processes. Table 1 shows the observed bands and the assignment corresponding to the 3*s*-*Rydberg* state, the bands of 4*s*-*Rydberg* state are not assigned.

4 Conclusions

Multiphoton ionization and fragmentation studies from 582.60 to 585.8 nm have been performed for acetone molecule using an optical parametric oscillator system coupled to time-of-flight mass spectrometer. We have identified three channels of dissociation of the acetone cation, the principal of these channels produce the acetyl ion and methyl radical. We have also observed the fragment COH^+ which can be originated by keto-enol

Table 1. Observed vibronic bands in the spectrum.

Vibronic band (cm^{-1})[a]	$\Delta\nu$	Assignment[b]
51204.5	0	Origin
51222.0	17.5	Non-assigned
51255.2	50.7	12_1^1
51265.8	61.3	17_1^1
51293.8	89.3	12_2^2
51336.0	131.5	Non-assigned
51346.5	142.0	Non-assigned
51385.5	181.0	17_0^1
51424.0	219.5	Non-assigned
51450.5	246.0	12_0^2

[a] Wavenumber in the vacuum, [b] assignment according to reference [8].

transformation of the acetone or acetyl ion. This is explained by observation of bimodal velocity distribution for $m/e = 43$ and 58 corresponding to CH_3CO^+/CH_2COH^+ and $CH_3COCH_3^+/CH_2C(OH)CH_3^+$, respectively.

We have also measured the origin bands of the $3s \leftarrow n$ and $4s \leftarrow n$ transition through three-photon and four-photon resonant ionization processes, respectively. In the wavelength range used it is not possible to fully resolve the vibrational transitions due to the $3s$- and $4s$-*Rydberg* interaction. Therefore we observe the mixture of the various vibrational bands of the $3s$ and $4s$-*Rydberg* states.

This work was performed with financial support from CONACYT and DGAPA-UNAM. The authors thank A. Bustos for technical support.

References

1. G.A. Gaines, D.J. Donalson, S.J. Strickler, V. Vaida, J. Phys. Chem. **92**, 2762 (1988)
2. D.J. Donalson, G.A. Gaines, V. Vaida, J. Phys. Chem. **92**, 2766 (1988)
3. R. McDiarmid, J. Chem. Phys. **95**, 1530 (1991)
4. J.G. Philis, L. Goodman, J. Chem. Phys. **98**, 3795 (1993)
5. S.A. Buzza, E.M. Snyder, W. Castleman Jr, J. Chem. Phys. **104**, 5040 (1996)
6. Q. Zhong, L. Poth, A.W. Castleman Jr, J. Chem. Phys. **110**, 192 (1999)
7. R. McDiarmid, A. Sabljic, J. Chem. Phys. **89**, 6086 (1988)
8. J.G. Philis, J.M. Berman, L. Goodman, Chem. Phys. Lett. **167**, 16 (1990)
9. T. Kandu, S.N. Thakur, L. Goodman, J. Chem. Phys. **97**, 5410 (1992)
10. X. Xing, R. McDiarmid, J.G. Philis, L. Goodman, J. Chem. Phys. **99**, 7565 (1993)
11. Y.F. Zhu, S.L. Allman, R.C. Phillips, W.R. Garret, C.H. Chen, Chem. Phys. **2**02, 175 (1996)
12. V. Galasso, J. Chem. Phys. **92**, 2495 (1990)
13. S.R. Gwaltney, R.J. Bartlett, Chem. Phys. Lett. **241**, 26 (1995)
14. M. Merchan, B.O. Roos, R. McDiarmid, X. Xing, J. Chem. Phys. **104**, 1791 (1996)
15. E. Mejía-Ospino, I. Alvarez, C. Cisneros, Rev. Mex. Fis. **50**, 170 (2004)
16. W.C. Wiley, I.H. McLaren, Rev. Sci. Instrum. **26**, 1150 (1955)
17. W.M. Jackson, D. Xu., J. Chem. Phys. **113**, 3651 (2000)
18. W.M. Trott, N.C. Blais, E.A. Walters, J. Chem. Phys. **69**, 3150 (1978)
19. C. Majumder, O.D. Jayakumar, R.K. Vatsa, S.K. Kulshreshtha, J.P. Mittal, Chem. Phys. Lett. **304**, 51 (1999)
20. M.A. Trikoupis, J.K. Terlouw, J. Am. Chem. Soc. **120**, 12131 (1998)
21. P. Mourgues et al., Int. J. Mass Spectrom. **210/211**, 429 (2001)